Modelling Simul. Mater. Sci. Eng. **4** (1996) 231–244. Printed in the UK

Molecular dynamics simulation of interaction of a dislocation array from a crack tip with grain boundaries

Y W Zhang and T C Wang

LNM, Institute of Mechanics, Chinese Academy of Sciences, Beijing 100080, People's Republic of China

Received 10 July 1995, accepted for publication 6 December 1995

Abstract. The interaction of a dislocation array emitted from a crack tip under mode II loading with asymmetric tilt grain boundaries (GBs) is analysed by the molecular dynamics method. The GBs can generally be described by planar and linear matching zones and unmatching zones. All GBs are observed to emit dislocations. The GBs migrated easily due to their planar and linear matching structure and asymmetrical type. The diffusion induced by stress concentration is found to promote the GB migration. The transmissions of dislocations are either along the matched plane or along another plane depending on tilt angle θ. Alternate processes of stress concentration and stress relaxation take place ahead of the pileup. The stress concentration can be released either by transmission of dislocations, by atom diffusion along GBs, or by migration of GBs by formation of twinning bands. The simulated results also unequivocally demonstrate two processes, i.e. asymmetrical GBs evolving into symmetrical ones and unmatching zones evolving into matching ones during the loading process.

1. Introduction

Since the pioneering work of Eshelby and co-workers [1] on the pileup of linear dislocation arrays, attempts have been made to model the failure and hardening behaviours of polycrystals in terms of the pileup of the dislocation arrays. The static distributions of linear dislocation arrays have been considered by Li [2], Huang and Gerberich [3] and Shiue and Lee [4]. The problems of dynamic formation of a pileup of dislocation array against an obstacle have been investigated by Kanninen and Rosenfield [5] and Yokobori and co-workers [6]. In these and other studies, it has been noted that the assumption that the obstacles are either sessile dislocations or stiff barriers and the employment of continuum mechanics concept are unrealistic at the pileup ends. It leads to high stress concentration which approaches or exceeds the theoretic strength. Although a viscous obstacle has been used by Gerstle and Dvorak [7], the structure of the obstacles still has not been fully considered. The experimental results have shown that the obstacles are often associated with the GBs [8–10]. Since the processes of dislocation absorption and transmission, diffusion, migration, cavitation, dynamic recrystallization and intergranular fracture of GBs are often observed during the impingement of dislocations on GBs [10–12, 8], it is inappropriate to take the obstacles simply as sessile dislocations or as stiff barriers against the movement of dislocations.

The experiments with bicrystals of nickel have been designed by Lim and Raj [8] to study the reactions between dislocations and GBs. It is shown that asymmetrical reactions appear to promote migration and cavitation, while the symmetrical reactions produce

0965-0393/96/020231+14$19.50

dynamics recrystallization. The role of interactions between slip dislocations and [110] tilt GBs in crack nucleation has been analysed by Yoo and King [12]. Their results show that dislocation absorption into the boundaries depends on orientation and elastic anisotropy and the fracture plane depends on the asymmetric or symmetric pileup of dislocations. The conditions for dislocation transmission through the GB and into the adjacent grain have been investigated by Livingston and Chalmers [11], Shen and co-workers [13] and Lee and co-workers [10]. Since the dislocation transmission process involves the dynamics of dislocation motion as well as the geometry of the slip at GBs, the criterion is difficult to establish accurately. Most of the previous work has involved the analysis of static situations where the lattice dislocations interact with the GB prior to observation, so the details of atom arrangements of GBs and dynamic behaviours of dislocations may be considered more reasonably by the molecular dynamics method.

During the past a few years, molecular dynamics simulations of dislocation emission from a crack tip have been carried out by Hoagland and co-workers [14], deCelis and co-workers [15], Cheung and Yip [16] and Zhang and co-workers [17] and those of GB atom structure have been carried by Wang and co-workers [18] and Balluffi and Bristowe [19]. The computational results now can be compared directly with experimental observations [20]. This situation provides a new perspective in the study of the interaction of the dislocations emitted from a crack tip with the GBs by the molecular dynamics method.

In the present paper, we devise an atom configuration to study the dynamic interactions of dislocations emitted from a crack tip with a GB by the molecular dynamics method.

So far, most research work has dealt primarily with a symmetrical configuration. However recent experimental observations [21] have shown that asymmetrical GBs are usually the ones which could play an important role in the mechanical properties of polycrystals. The asymmetric $\langle 112 \rangle$ tilt GBs are used in the present simulations.

In the next section, we will describe the molecular dynamics method used in the present simulation, which includes the potential, boundary conditions, geometry and calculative method; in section 3, the simulated results are presented; in section 4 a discussion is given and finally, in section 5, some conclusions are presented.

2. Calculation method

2.1. Interatomic potential

The interatomic potential used here is the 'N-body' potential proposed by Finnis and Sinclair [22] and constructed by Ackland and co-workers [23]. The total energy takes the form of

$$E_{tot} = -\sum_i \rho_i^{\frac{1}{2}} + \frac{1}{2}\sum_i \sum_{j(i\neq j)} V_{ij} \tag{1}$$

where ρ is the second moment of the density of states, and

$$\rho_i = \sum_{j(i\neq j)} \Phi_{ij}. \tag{2}$$

V_{ij} and Φ_{ij} are functions only of the interatomic distance. The function forms for Cu can be found in [23].

2.2. Method of solution

The inner atoms follow the Newton law

$$\boldsymbol{F}_i = -\frac{\partial E_{tot}}{\partial \boldsymbol{r}_i} = m_i \dot{\boldsymbol{v}}_i. \tag{3}$$

The present molecular dynamics calculations are carried out by the Leapfrog Algorithm as follows

$$\begin{cases} \boldsymbol{v}_i\left(t+\dfrac{\Delta t}{2}\right) = (1-\eta)\boldsymbol{v}_i\left(t-\dfrac{\Delta t}{2}\right) + \dfrac{\boldsymbol{F}_i}{m_i}\Delta t \\ \boldsymbol{r}_i(t+\Delta t) = \boldsymbol{r}_i(t) + \boldsymbol{v}_i\left(t+\dfrac{\Delta t}{2}\right)\Delta t. \end{cases} \tag{4}$$

In (3) and (4), m_i is the mass of the ith atom, η is the numerical damping parameter which is taken to be 0.1 for relaxation processes and zero for loading processes. The above scheme provides an update formulation from the current time t. The time step in the present calculation is taken to be 1.18×10^{-14} s and loading rate is $\dot{K}_{II} = 0.0874$ MPa m$^{1/2}$ ps^{-1}. For the relaxation process, after 500 time steps the initial temperature of the systems is taken to be near 0 K. For the loading process, 2000 time steps are used.

The atomic level stress associated with atom i can be calculated by the following formula [17]:

$$\sigma^i_{\alpha\beta} = \frac{1}{2\Omega^i}\left[\sum_j V'(r^{ij}) - \rho_i^{-\frac{1}{2}}\sum_j \Phi'(r^{ij})\right]\frac{r^{ij}_\alpha r^{ij}_\beta}{r^{ij}} \tag{5}$$

where Ω^i is the volume of atom i, r^{ij} is the distance between atom i and j and the prime $'$ denotes the derivative with respect to r^{ij}.

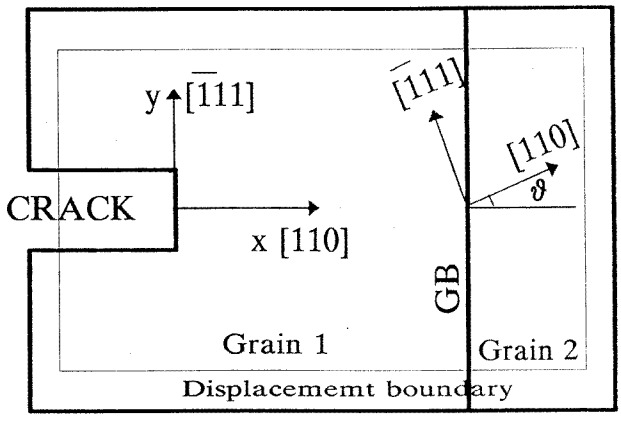

Figure 1. Schematic diagram for the simulated atom model; the crack is in grain 1, the common tilt axis is [1$\bar{1}$2] and the tilt angle is θ.

After the relaxation with prescribed displacement boundaries, the residue stresses of the inner atoms can be calculated through equation (5). Similarly, the stresses at the loading stage can also be calculated by equation (5).

2.3. The atom lattice geometry

A parallelepiped with a slit is used as the simulated cell in the present calculations as shown in figure 1. The grain 1 is so arranged that its [110], [$\bar{1}$11] and [1$\bar{1}$2] directions are along x,

y and z respectively. The distance between the crack tip and GB is $168 \times \frac{\sqrt{2}}{4}a_0$ (a_0 is the lattice constant). The tilt axis is $[1\bar{1}2]$ and the tilt angle is θ. The GB is the asymmetrical tilt one and the GB plane is selected to be (110) in grain 1. The length of the simulated cell in x-direction is $280 \times \frac{\sqrt{2}}{4}a_0$ and the width in the y-direction is $101 \times \frac{\sqrt{3}}{3}a_0$. The distance between the crack tip and the left boundary is $56 \times \frac{\sqrt{2}}{4}a_0$. The separation between the upper and lower crack planes is $\sqrt{3}a_0$, which is larger than $1.22a_0$, the cutoff distance of the potential. The number of atoms used in the present simulations for each case is about 28 890. Since a period with six layers and periodic conditions along $[1\bar{1}2]$ are used, the nucleation and motion of partial dislocations can be described with the present lattice configuration.

The cell containing the chosen CSL boundary is constructed first, and then an equilibrium relaxed structure is built up by minimizing the total energy with respect to all atomic position subject to the prescribed displacement boundaries.

Since the lattice configuration projected on the $(1\bar{1}2)$ modelling plane is a square structure, the emitted dislocations have a very simple core structure on the modelling plane. Accordingly, positions of the emitted dislocations can identified easily by determining the extra-half atomic planes.

2.4. The boundary conditions

The border discrete atoms of the simulated cell are prescribed by the mode II anisotropic elastic K displacement field [24] by using the elastic constants of grain 1 for simplicity.

The treatments of boundary conditions are of crucial importance to the accuracy of the final results as pointed out by deCelis and co-workers [15]. The displacement boundaries suffer serious deficiency when dislocations arrive the borders, because there is no way for the dislocations to penetrate the boundaries. In the present simulation, such a deficiency is partially overcome by locating a GB ahead of the crack tip. Hence the dislocations emitted from the crack tip will directly interact with the GB. Since the GB deformation processes are very complicated, it is impossible to determine the displacement boundaries accurately. But since the crack tip and the pileup end are relatively far from the prescribed displacement boundaries, the boundary effects are relatively small.

3. Simulated results

Several cases with variation of misorientation of high-angle grain boundaries have been investigated. Those selected to be reported are chosen on the basis that they provide new and relevant information. The atom configuration figures are plotted on the projected $[1\bar{1}2]$ plane with a period of six layers.

3.1. The case with $\theta = 70^\circ$

The GB is of a random high-angle asymmetry and the relaxed GB does not exhibit the initial type. Some of the {111} planes in the two grains become matched over the GB. The residual stresses near the simulation cell border, at the GB and at the crack tip after the relaxation process are examined. It is shown that the potential used here well characterizes the lattice equilibrium at ground state and therefore the residual stress near the border is very small and can be neglected. The stress at the crack tip is also low and the crack tip configuration does not change apparently before and after the relaxation process. After the relaxation or

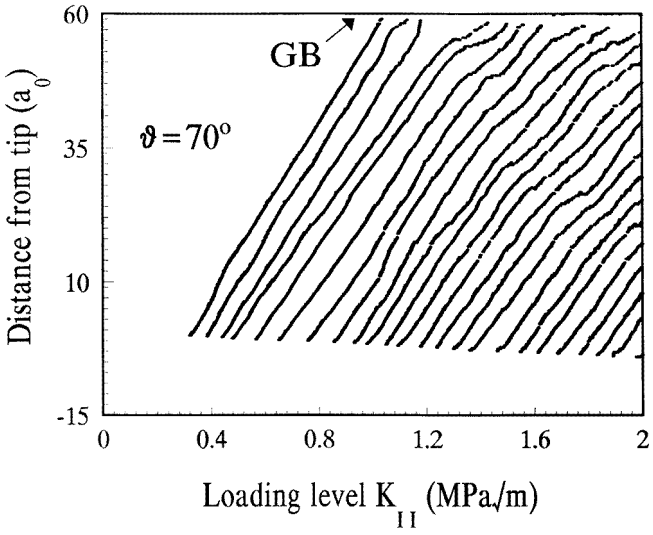

Figure 2. The curves of the distance moved by the emitted dislocations against the loading level K_{II} are given. When loading increases, the dislocations are nucleated in a sequential order and move away from a crack tip. The GB is approximately $60a_0$ ahead of the crack tip. From this figure the repulsion and attraction of the GB to the dislocations can be seen.

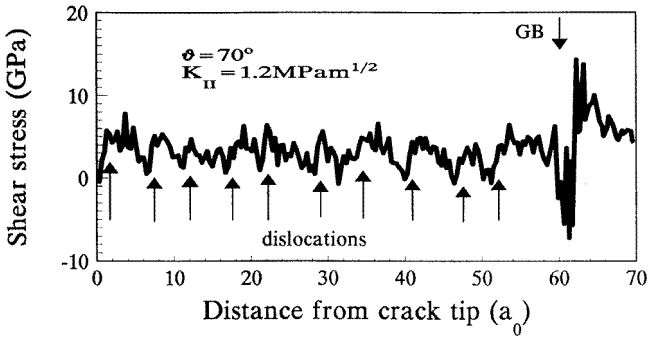

Figure 3. Stress distribution along the prolongation of the crack plane after the GB has absorbed three dislocations. The position of the GB is indicated by the down arrow, the stress distribution at the GB is similar to that of a dislocation with a large Burgers vector. Between the crack tip and the GB, there are ten dislocations as indicated by up arrow.

at initial loading stage, the residue stress at GB is low too; this may be the reason why the atoms in GB accommodate each other to reduce the stress level. After the loading is applied, the GB structure begins to evolve with the loading. Some parts of the GB evolve into the symmetrical type and the GB itself becomes zigzag. Emission of dislocations from the GB into grain 1 is also observed. With increasing loading level, the dislocations emitted from the GB begin to move towards the crack tip; meanwhile dislocations emitted from the crack tip begin to slide away from a crack tip. The positions of dislocations emitted from the crack tip along [110] in grain 1 against loading level are given in figure 2. From this figure, it can be seen that the first partial dislocation is emitted at 0.32 MPa $m^{1/2}$ and subsequently moves from away from the tip. With increase of loading, more dislocations are emitted and

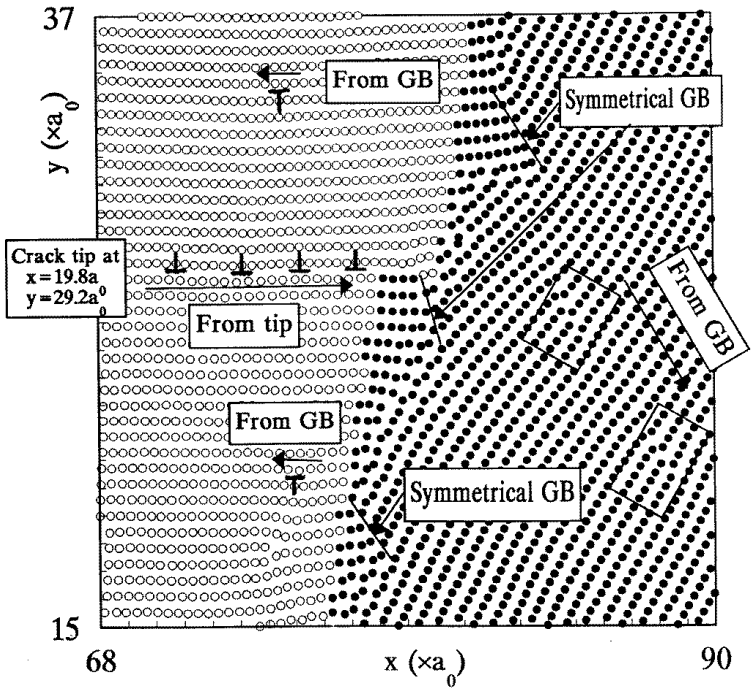

Figure 4. The atom configuration for $\theta = 70^\circ$ at $K_{II} = 2.0$ MPa $m^{1/2}$. Migration in some parts of the GB, emission and transmission of dislocations can be observed clearly.

thereafter move away from the crack tip. The moving speed of these emitted dislocations almost keeps constant at the initial stage. The leading dislocation almost keeps a constant speed even when it approaches the GB (the GB is approximately at $60a_0$ ahead of the crack tip) and then it is absorbed by the GB. But the second partial is repelled by the GB, while the third partial accelerates to move toward the GB. After absorption of the three partial dislocations, the GB seems to become saturated and it strongly repulse the fourth partial and the following dislocations. The moving speed of the following dislocations becomes heterogeneous near the GB. This may be the result of dynamical pileup of the dislocations near GB. The stress distribution along the prolongation of the crack plane is shown in figure 3, where three partial dislocations emitted from the crack tip are absorbed by the GB. It is shown that the crack tip stress level is low due to the strong shielding effect of the emitted dislocations indicated by the up arrows in figure 3. Although there are some oscillating effects resulting from the atom vibration, the simulated stress distribution at the dislocation core can still be observed to have some similarity with the crystal dislocation. The stress distribution at the GB indicated by a down arrow in figure 3 exhibits a shape similar to that of a large Burgers vector. Due to the strong stress concentration ahead of the pileup GB migration takes place. The GB becomes more zigzag and more parts of the GB become symmetrical as shown in figure 4. Two dislocations are found to be emitted from the GB into grain 2 to relax the stress concentration ahead of the pileup. After deformation, more {111} planes of two grains are in register over the GB. Although at this loading stage the GB structure and shape are changed greatly and the atomistic processes are very complicated, no cracks or voids are found in this case.

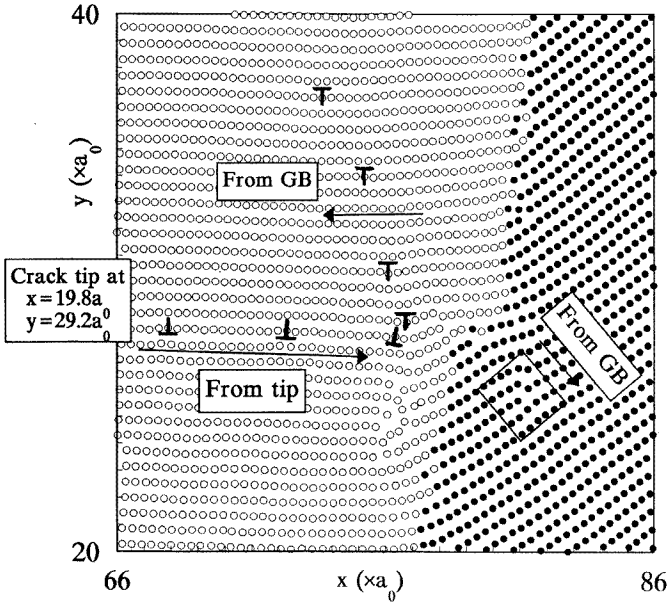

Figure 5. The atom configuration for $\theta = 44.415^\circ$ at $K_{II} = 1.8$ MPa $m^{1/2}$. Emission and transmission of dislocations can be observed. More {111} planes in the two grains become matched.

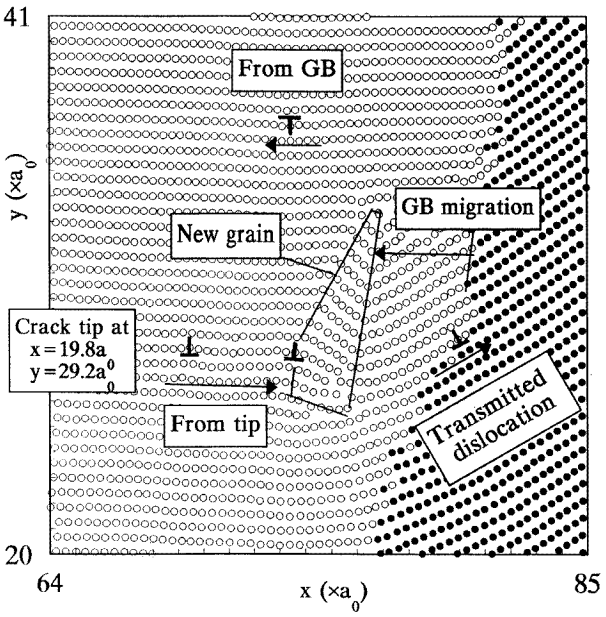

Figure 6. The atom configuration for $\theta = 44.415^\circ$ at $K_{II} = 2.0$ MPa $m^{1/2}$. GB migration and an intermediate grain can be observed.

3.2. The case with $\theta = 44.415^\circ$

The GB with 44.415° is a coincident site lattice (CSL) GB with Σ21. After relaxation, the GB does not keep its initial CSL type and becomes slightly zigzag. Some parts of the GB

also evolve into the symmetrical ones. The {111} planes of the two grains are in register over some parts of the GB to form the matching zones. After the loading, more parts of the GB evolve into symmetrical ones due to migration. Before the leading dislocation emitted from the crack tip reaches the GB, no dislocation is observed to be emitted from the GB. After the impingement of the dislocations emitted from the crack tip, some dislocations are emitted from the GB far from the pileup site and the GB becomes even more zigzag. With the increase of loading, more dislocations are emitted from the GB into grain 1. The emitted partial dislocations attached to the GB with an stacking fault arrange themselves to form a low-angle GB (see figure 5). Due to the impingement, the part of the GB below the pileup begins to migrate towards the crack tip. In order to relax the stress concentration ahead of the pileup, dislocations are transferred through the GB into grain 2 either along a slip system on matched planes or along another slip system on another plane as shown in figure 5. Due to the serious pileup of dislocations, the density of atoms below the pileup dislocations is lower than above, therefore a lattice instability induced by higher stress takes place; meanwhile a small grain is nucleated as shown in figure 6. After serious deformation, the {111} planes of the adjacent grains match very well over most parts of the GB.

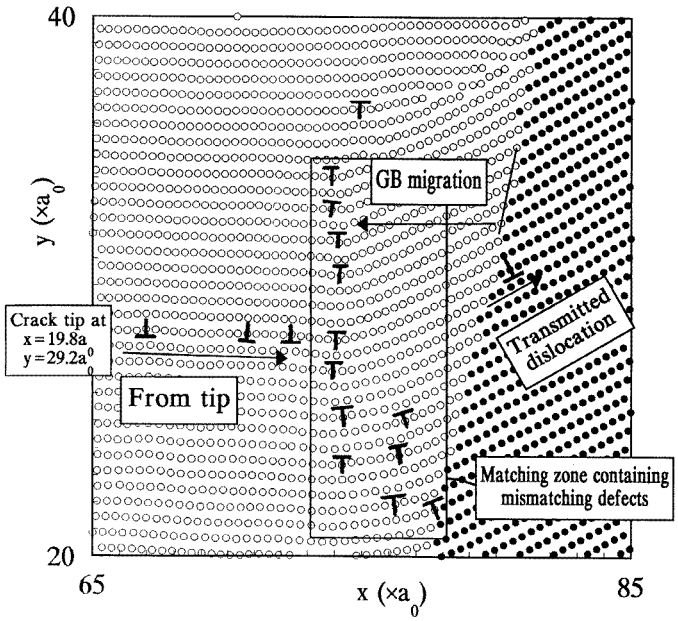

Figure 7. The atom configuration for $\theta = 35^\circ$ at $K_{II} = 1.8$ MPa $m^{1/2}$. GB migration and dislocation transmission can be seen. Mismatching plane defects climb to form a low-energy structure. More parts of the GB become well matching zones. The misorientation of the GB after migration decreases.

3.3. The cases with other θs

For $\theta = 35^\circ$, dislocation emissions from the GB into grain 1 are observed before impingement and some parts of the GB migrate to form a symmetrical tilt GB. After absorption of four partial dislocations emitted from the crack tip, the GB repels the subsequent dislocations. With the increase of loading, more {111} planes of adjacent grains

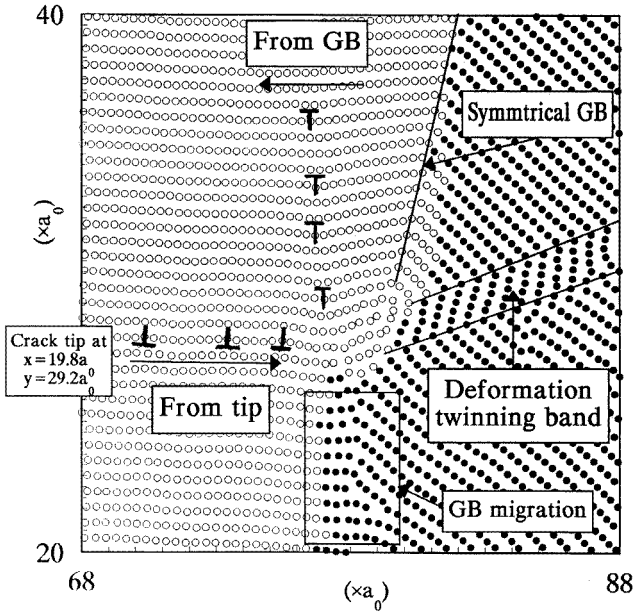

Figure 8. The atom configuration for $\theta = -35^\circ$ at $K_{II} = 2.0$ MPa $m^{1/2}$. GB migration, GB dissociation and twinning deformation can be observed.

become matched over the GB. Diffusion and dislocation emission induced relaxation of stress concentration ahead of the pileup are observed. Due to the migration of the GB, the tilt angle between adjacent grains begins to decrease (figure 7). For $\theta = -35^\circ$, atoms in the GB begin to reorganize and to form matched planes and lots of dislocations are emitted from the GB during loading. Some parts of the GB migrate right to form a symmetrical tilt GB. After absorbing two leading partials emitted from the crack tip, a partial dislocation is emitted from the pileup end into grain 2. The residual dislocations resist further emission along this path. The stress concentration ahead of pileup relaxes by diffusion along the GB and results in the migration of the GB to form a large part of symmetrical tilt GB; meanwhile several dislocations are emitted from the GB to form a low-angle GB. Hence a GB may dissociate into two parts, one of which is a symmetrical GB and the other is a low-angle GB. When $K = 2.0$ MPa $m^{1/2}$, the stress concentration ahead of the pileup relaxes by forming a deformation twinning band (figure 8).

For the $\theta = 101.53^\circ$ $\Sigma 5$ GB, a void and a small grain are observed (figure 9). It seems that the nucleation of the void results from the diffusion induced by the high stress gradient and the small grain results from the dissociation of the GB.

4. Discussion

4.1. Atomic structure of the GBs

Since the intersecting line of the {111} planes in grain 1 and grain 2 is parallel to the tilt axis, the atomic densities in this aligned planes are high and their interaction across the plane is strong. Hence this kind of GB easily forms a matched plane [25, 26]. The present simulations show that, as well as the planar matching over the GB, there is also

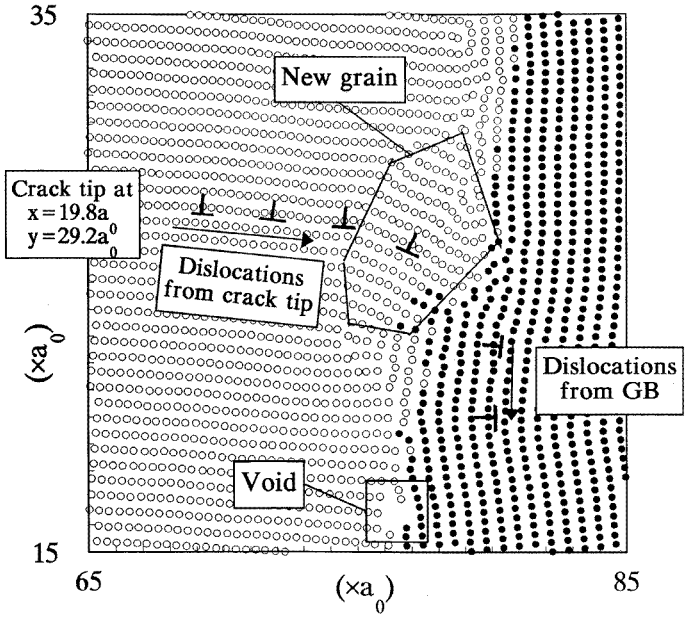

Figure 9. The atom configuration for $\theta = 101.53^\circ$ at $K_{II} = 2.0$ MPa $m^{1/2}$. GB migration, an intermediate grain, dislocation transmission and a void can be observed.

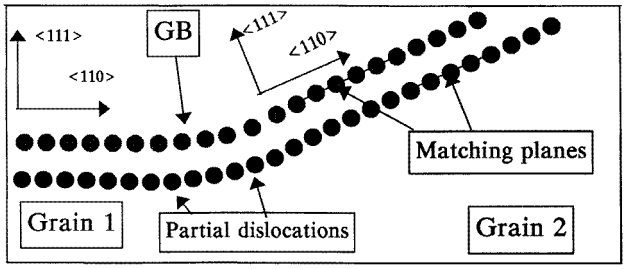

Figure 10. One type of in-matching-plane defect similar to a perfect dislocation in an FCC crystal. The two Shockley dislocations only dissociate slightly.

linear matching along the closely packed direction on the matched planes. We call this kind of GB the planar and linear matching GBs. The present simulations also show that the lower the GB tilt angle, the higher the planar and linear matching. When $\theta < 30^\circ$, the initial relaxed GB can be well characterized by the planar and linear matching model. In the matching zones, an array of edge character Van der Merwe dislocations with their lines along the tilt axis and their Burgers vectors along $\langle 111 \rangle$ on the GB plane are observed. The average separation of these two adjacent dislocations is

$$f_{ave} = \frac{\sqrt{3}a_0}{3(1 - \cos\theta)}. \tag{6}$$

In the matched planes, two kinds of dislocation structure in GBs are observed. The first contains two Shockley partial dislocations whose Burgers vectors are in the matched plane in grain 1 and grain 2 respectively. These two partials either do not dissociate or dissociate

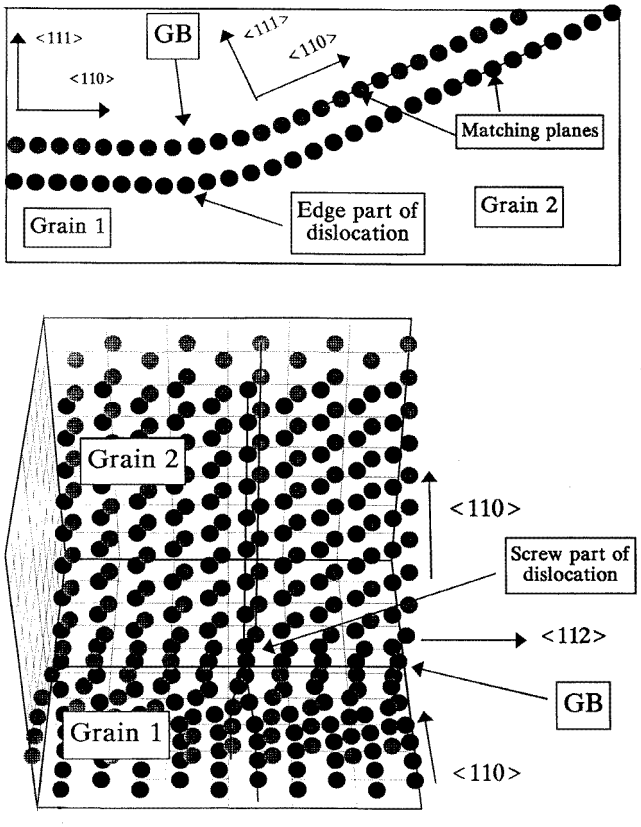

Figure 11. The other type of in-matching-plane defect. It contains a edge component with Burgers vector $\frac{1}{4}\langle 110\rangle$ as shown in (a), and a screw component with Burgers vector $\frac{1}{4}\langle 112\rangle$ as shown in (b).

only slightly (figure 10). The other contains a mixed dislocation which consists of an edge component $\frac{1}{4}\langle 110\rangle$ and a screw component $\frac{1}{4}\langle 112\rangle$ (figure 11). Both Van der Merwe dislocations and dislocations with the screw component result in stacking faults over GBs. For $\theta > 30^\circ$, with the increase of tilt angle θ, the matching zones become fewer meanwhile the bad misfit zones in the GB increase. We call the misfit zones in GBs the unmatching zones, in which atomic structures are irregularly stacked. When loading is applied, atoms in high-angle GBs begin to reorganize and gradually to form matching zones. Although the initial GB configurations are given by CSL, the relaxed GBs are not of CSL, but of planar and linear matching and/or unmatching types. When θ is large enough, $\{110\}_1\theta/\langle 112\rangle$ GBs are composed of matching zones where there exist mismatching defects and unmatching zones where the atoms are stacked irregularly.

4.2. GB as dislocation sources

In the present simulations, the GBs are observed to emit dislocations into grain 1 along a slip system moving towards crack tip before impingement of dislocation emitted from the crack tip. This is because the slip system with the highest Schmid factor is the most favourable. These dislocations emitted from GBs into grain 1 are partial dislocations. We also find that

dislocations emitted are generally from the matching zones. A detailed examination shows the emitted dislocations are just the dislocations in the matching GB zones as discussed in subsection 4.2. The unmatching zones emit dislocations with more difficulty than matching zone does. When the loading is applied, the two Shockley dislocations (figure 10) begin to dissociate; one partial is emitted from the GB into grain 1 and leaves a stacking fault between the emitted partial and the remained partial in GB. If the mixed dislocation (figure 11) is loaded, it can also be emitted from the GB into grain 1. This GB structure explains why so many dislocations are emitted from the GB. The impingement of the dislocation array emitted from the crack tip on GBs is also observed to emit dislocations. This process relaxes the stress level ahead of the pileup. GBs acting as sources of lattice dislocations have also been observed in the experiments of Malis and Tangri [27] and Elkajbaji and Thibault-Desseaux [28]. Their results have shown that the dislocation density near the GB is higher than in the interior of the crystal during the initial deformation stage, for the activation of GB sources produces dislocations that are confined to the boundary zone and the presence of GB dislocations is a favourable boundary activation source. Their results also showed that the ejection of partial dislocations into the opposite grain, caused by dislocation pileup, was observed fairly often and the emitted partials remained attached to the GB with a stacking fault. These experimental results are consistent with the present simulation.

4.3. GB migration

Our simulated results show that GB migration strongly depends the GB structure. The GB migration takes place easily in matching zones. This is because the dislocations in the matching zones move easily and therefore promote the GB migration. In addition, the GB migration tends to change the asymmetrical GBs into the symmetrical ones. This means the symmetrical tilt GBs are more stable than the asymmetrical ones. The experimental results of Lim and Raj [8] have shown that the migration of asymmetrical GBs is considerable and the shape of the boundary after migration becomes zigzag. These results are consistent with our present simulations. Migration induced by diffusion along the GB is observed in the cases of $\theta = 70^\circ$ and -35°. Such diffusion mainly results from the strong stress concentration ahead of the pileup. The experimental observation of Jahn and King [30] has shown that extensive diffusion induced GB migration has occurred and that the GB has taken up a zigzag morphology. This is also in agreement with our simulated results.

4.4. Dissociation of GB

GB dissociations are observed in several cases in our simulation. It is shown that a GB may dissociate into two components, one of which may be a symmetrical tilt GB and the other may be a low-angle GB (figure 7). In these processes, dislocations are often ejected from the asymmetrical GB first, and then the asymmetrical GB begins to evolve into a symmetrical one. The experimental observation of Jahn and King [30] has shown that the GB starts to move only after ejecting arrays of dislocations. This result is consistent with some of our simulations. A more complicated dissociation of the GB can also take place as shown in figure 9, in which a small grain may be nucleated. Similar phenomena are also observed in the experiment by Forwood and Clarebrough [29]. Their experimental results show that an asymmetrical tilt GB may dissociate and a new intermediate grain is nucleated. Such a scenario is in agreement with some of our simulated results. Accordingly, the asymmetrical GBs are generally more unstable than the symmetrical ones.

4.5. Transmission of dislocations

Our simulations show that the tilt angle θ is an important parameter to control the dislocation transmission process at the GB. The smaller θ, the easier the dislocation transmission. When θ is smaller than 50°, the dislocations ahead the pileup may transfer through the GB from grain 1 into grain 2 along the matched planes. The residual dislocations left by the dislocation transmission in the GB will inhibit further transmission along this path; therefore the passage of the subsequent dislocations may be along another slip plane. When θ is greater than 50°, the dislocation transmission is generally not along the matched plane, but along another slip plane. This is because the Burgers vector of the residual dislocations is too large when θ is high. The transmission processes have also been experimentally observed by many researchers [4, 12, 28]. Their results show that the passage of a dislocation depends on the residual dislocation and initial and the final slip planes. We find that at least a pair of Shockley dislocations of the leading perfect dislocation are merged into the GB, transmission of dislocation may take place.

4.6. Relaxation of stress concentration

The pileup of dislocations at the GB leads to complicated atomistic processes. The present simulations show that the stress concentration can be relaxed either by dislocation emission into the adjacent grain, by atomic diffusion along the GB which may result in GB migration, directly by migration or by formation of a twinning band. These different processes may take place at different stages of the same deformation process or at different tilt angle. Hence the interaction of an array of pileup dislocations with a GB is an alternative process between pileup and relaxation. These processes may be suitable for the pileup of dislocations at any kind of high-angle GB.

4.7. Cavitation during impingement

In all present simulations, only the $\theta = 101.53^\circ$ $\Sigma 5$ GB is found to form a void; this void is not just at the impingement site and seems to result from the diffusion induced by the high stress gradient. In other cases, no cavitation is observed. It seems that this kind of GB in Cu can accommodate themselves to prohibit cracking and voiding by migration and diffusion. The experimental results [8] show that cavitation and migration are inversely related, i.e., in regions where migration has occurred there is little cavitation and vice versa. This is consistent with the present results.

5. Conclusions

By means of the MD simulation method, the interaction of dislocations emitted from a crack tip with an asymmetrical tilt GB is analysed numerically. We have found that the $\{110\}_1\theta/\langle 112\rangle$ GBs can be described by a planar and linear matching model when $\theta < 30^\circ$. When $\theta > 30^\circ$, the GBs consist of both matching zones and unmatching zones where the GB atoms are irregularly stacked. With the increase of loading, the size and number of matching zones increase. The asymmetrical tilt GBs are found to be unstable and can migrate into symmetrical ones and result in zigzag shape of GBs. The GBs may also dissociate into two parts, one of which is symmetrical and the other is of low-angle character. During the loading process, both crack tip and GB are capable of emitting dislocations. A pileup of dislocations emitted from the crack tip can be built up after the impingement of the

dislocation on GB. Ahead of the pileup, two processes, i.e. pileup and relaxation, take place alternately. The relaxation processes may be dislocation transmission, diffusion along GB, migration and formation of twinning bands. In addition, recrystallization and cavitation may also take place ahead of the dislocation pileup.

Our present analysis is only a preliminary work. Since the interactions of pileup dislocations with GB are very complicated processes, which involve many different events and deserve more comprehensive investigation, more efforts are needed. Future work should be focused on the significant effect of thermal activation on the interaction of dislocations with GBs and the employment of more accurate boundary conditions. Further detailed investigation on the influences of tilt angle and tilt axis are also needed. Furthermore the simulated results should compare with analytical results or experimental observations in more detail.

Acknowledgment

The project is supported by the National Natural Science Foundation of China.

References

[1] Eshelby J D, Frank F C and Nabarro F R N 1951 *Phil. Mag.* **42** 351
[2] Li J C M 1986 *Scr. Metall.* **20** 1477
[3] Huang H and Gerberich W W 1992 *Acta Metall. Mater.* **40** 2873
[4] Shiue S T and Lee S 1993 *Phil. Mag.* A **67** 1433
[5] Kanninen M F and Rosenfield A R 1969 *Phil. Mag.* **20** 569
[6] Yokobori A T, Isogai T and Yokobori T 1993 *Acta Metall. Mater.* **41** 1405
[7] Gerstle F P and Dvorak G J 1974 *Phil. Mag.* **29** 1337
[8] Lim L C and Raj R 1985 *Acta Metall.* **33** 2205
[9] Miura S and Saeki Y 1978 *Acta Metall.* **26** 93
[10] Lee T C, Robertson I M and Birnbaum H K 1990 *Metall. Trans.* A **21** 2437
[11] Livingston J D and Chalmers S B 1957 *Acta Metall.* **5** 322
[12] Yoo M H and King A H 1990 *Metall. Trans.* **21A** 2431
[13] Shen Z, Wagoner R H and Clark W A T 1986 *Scr. Metall.* **20** 921
[14] Hoagland R G, Daw M S, Foiles S M and Baskes M I 1990 *J. Mater. Res.* **5** 313
[15] deCelis B, Argon A S and Yip S 1983 *J. Appl. Phys.* **54** 4864
[16] Cheung K S and Yip S 1990 *Phys. Rev. Lett.* **65** 2804
[17] Zhang Y W, Wang T C and Tang Q H 1995 *J. Appl. Phys.* **77** 2393
[18] Wang G J, Sutton A P and Vitek V 1984 *Acta Metall.* **32** 1093
[19] Balluffi R W and Bristowe P D 1984 *Surf. Sci.* **144** 28
[20] Cosandey F, Chan S W and Stadelmann P 1990 *Metall. Trans.* A **21** 2299
[21] Randle V 1994 *Acta Metall. Mater.* **42** 1769
[22] Finnis M W and Sinclair J E 1984 *Phil. Mag.* **50** 45
[23] Ackland G J, Tichy G, Vitek V and Finnis M W 1987 *Phil. Mag.* A **56** 735
[24] Sih G C and Liebowitz H *Fracture: an advanced treatise* vol 2, ed H Liebowitz (New York: Academic) p 67
[25] Pumphrey P H 1972 *Scr. Metall.* **6** 107
[26] Ralph B, Howell P R and Page T F 1973 *Phys. Status Solidi* b **55** 641
[27] Malis T and Tangri K 1979 *Acta Metall.* **27** 25
[28] Elkajbaji M and Thibault-Desseaux J 1988 *Phil. Mag.* A **58** 325
[29] Forwood C T and Clarebrough L M 1984 *Acta Metall.* **32** 757
[30] Jahn R J and King A H 1992 *Acta Metall. Mater.* **40** 551